Self-organized multigrain patterning with special grain boundaries produced by phase transformation cycling

Yipeng Gao, Yongfeng Zhang, Benjamin W. Beeler, and Yunzhi Wang

Self-Organized Multi-Grain Patterning with Special Grain Boundaries Produced by Phase Transformation Cycling

Yipeng Gao[a,b*], Yongfeng Zhang[b], Benjamin W. Beeler[b], Yunzhi Wang[a*]

[a] *Department of Materials Science and Engineering, The Ohio State University, Watts Hall, 2041 College Road, Ohio 43210, United States.*
[b] *Department of Fuel Modeling and Simulations, Idaho National Laboratory, 2525 Fremont Avenue, Idaho 83415, United States.*

Abstract

In crystalline solids, grain boundaries (GBs) play a significant role in determining a large number of material properties. The design and synthesis of special GBs has been a long-standing challenge in materials science and engineering. Here we demonstrate a new mechanism to produce special GBs. Unique multi-grain structures can be obtained through cyclic, diffusionless phase transformations under external fields, with all GBs being coherent special GBs. The crystallographic character of the GBs produced in this way is dictated by the broken symmetry during the phase transformations, while the topology of the GB network is determined by the geometric compatibility and self-organization of the multi-grain structures. Such a new mechanism not only suggests a novel method of GB engineering, but also reveals a fundamental relationship between special GBs and phase transformations from a crystallographic point of view.

Introduction

In materials science and engineering, extensive attentions have been given to grain boundaries (GBs) because of their critical importance in determining material properties [1-6]. As a consequence, a number of processing techniques have been developed to tailor material properties through GB engineering. For example, grain refinement is one of the most efficient ways of strengthening according to the Hall-Petch equation [7, 8], which leads to an excellent combination of strength and ductility. Special thermodynamic and kinetic phenomena are also widely observed near GBs, e.g., GB segregation (including segregation transition) [9] and GB diffusion, which are exclusively contained in GBs and do not exist in the bulk. In the emerging field of GB engineering, GBs are optimized for desired material properties. Two basic characters of GBs considered in GB engineering are (1) the crystallographic and geometric features of GBs, e.g., misorientation and inclination and, (2) the topology of the GB network [2-4, 10]. As discovered in experiments, unique properties can be associated with the so-called special GBs [1, 11]. From a crystallographic point of view, special GBs (also called Σ GBs sometimes) are

---

usually featured by specific values of misorientation that allow atomic sites from neighboring lattices of adjacent grains to coincide, and the reciprocal density of coinciding sites is designated as Σ. For a given misorientation, a special GB can be either coherent if the boundary plane is low-index (i.e., all lattice planes are continuous from one grain to the other across the GB), or incoherent if the boundary plane is irrational (usually high index in experiments). Coherent special GBs can exhibit sharp extrema for a number of orientation-dependent properties. These properties, including GB energy and mobility, fracture toughness, diffusivity, defects migration rate and corrosion resistance, are usually distinctive at various types of coherent special GBs [11].

Topology of GB network (or GB network connectivity) is another critical factor not only determining the thermodynamic stability and the evolution of GB network but also affecting several material properties [4, 10]. For example, the branching features of the network (i.e., grain junctions and nodes) control diffusion, corrosion and oxidation behavior, and environmental-assisted inter-granular crack propagation caused by the transport along GBs. In addition, as reported in the literature, a reasonable balance of strength and ductility can be achieved by introducing ultra-fine isolated grains into a matrix grain, which also suggests a critical link between unique topology of GB network and material properties [12]. However, despite their importance, the above two characters are usually difficult to control precisely in GB engineering. One conventional technique of GB engineering is the production of annealing twins through iterative cold working and annealing, where the proportion of special twin boundaries could be over 60% including both coherent and incoherent twin boundaries. Another technique is pulsed electrodeposition, which can produce lamellar structures with a large amount of $\Sigma 3$ coherent twin boundaries [13]. However, most of the existing GB engineering techniques can only be applied to the coherent $\Sigma 3$ GB in face-centered-cubic (FCC) crystals, because the grain boundary energy of this specific type is much lower than those of other candidate GBs in FCC. To the best of our knowledge, a general approach to precisely design other coherent GBs (e.g., $\Sigma 5$ and $\Sigma 7$) in FCC materials or coherent special GBs in other crystal systems, e.g., body-centered cubic (BCC) and hexagonal close-packed (HCP) structures, is still unavailable.

Since the characters of GBs are difficult to precisely control in the diffusional processes (e.g., annealing) discussed above, it is natural to consider the possibility of utilizing *diffusionless* processes. In fact, it is recently reported that crystalline defects, such as dislocations and special GBs, can be produced by the diffusionless phase transformations in which the symmetry groups of the parent and product phases cannot be included in a common finite group [14]. However, because such phase transformations are beyond the reach of Landau's classical phase transition theory [14, 15], the formation mechanism of transformation-induced defects is still unclear due to the lack of a mathematical tool. In particular, it has not been well recognized that *special GBs are intrinsically associated with the broken symmetry during phase transformation cycling*. During this process, a large number of crystallographically equivalent structural states, not confined in a single Ericksen-Pitteri neighborhood (EPN) [14, 16], can be generated through

transformation cycling, which provides plenty of fundamental building blocks for GB design. EPN is a neighborhood surrounding a unique high symmetry structural state (e.g., the structural state of the parent phase) in the deformation space (or strain space). Within the EPN, all the other states have relatively low symmetry comparing with the high symmetry state [14]. In other word, considering a continuous deformation process from the high symmetry state to any other state in the EPN, we only expect the loss of symmetry operations (a group-subgroup relation between the symmetry groups of the initial and final states). Note that GBs generated by transformation cycling is distinctively different from the twin boundaries produced by one-way transformation, because the latter is always confined in a single EPN while the former could involve a few different EPNs. As will be shown in the following, by employing a newly developed theoretical framework, i.e., phase transition graph (PTG) [17], we can systematically determine the special GBs generated during diffusionless phase transformation cycling where all of the structural states (as well as domain states) and GBs self-organize into a special polycrystalline aggregate.

In this work, inspired by recent experimental observations of transformation-induced GBs and self-accommodated multi-domain structures [18-20], we propose a new means to design and develop multi-grain structures through diffusionless phase transformation cycling. All GBs produced in this way are coherent special GBs, the types of which are dictated by the broken symmetry during the phase transformations. The topology of GB network is dictated by geometric compatibility and self-organization of multi-grain structures. To illustrate the generic mechanism, a phase transformation from square lattice to hexagonal lattice in 2-dimensional (2D) is analyzed first. It is shown that the GBs generated during a transformation cycle are $\Sigma 5$ boundaries. Purely from crystallographic point of view, we demonstrate that a multi-grain pattern with all $\Sigma 5$ boundaries and a unique topology of GB network, i.e., isolated small grains embedded in one matrix grain, could be generated during a transformation cycle. A similar mechanism is also found in Ti and Zr alloy systems undergoing the transformation cycling between BCC and HCP, in which the targeted multi-grain structures can be controlled through applying an external field, i.e., stress field. By applying a uniaxial compression during transformation cycling, we design a unique self-organized cross-twin structure (twins within twins) with $\Sigma 3$ and $\Sigma 7$ boundaries, the stability of which is demonstrated by both crystallographic analysis and phase field simulations. The size of the grains produced in this way is determined by the interplay between GB energy and elastic interaction, which is typically in the nano/submicro-scale.

Construction of Phase Transition Graph

Mathematically, a phase transformation between two structural states (the two states usually belong to two phases) can be interpreted as a pairwise relation and represented conveniently by a graph. For a PTG, $G(V, E)$, $V = \{v_{\alpha 1}, v_{\alpha 2}, \ldots, v_{\beta 1}, v_{\beta 2}, \ldots \}$ is a set of vertices that correspond to different structural states of α, β, ... phases, and E is a set of edges that connect the vertices

(describes transformation pathways among different structural states). To illustrate PTG construction at an intuitive level, we first consider a typical structural phase transformation in 2D between square and hexagonal lattices with the lattice correspondence shown in Fig. 1. According to the group theory [21], the transformation from square to hexagonal generates two variants, while that from hexagonal to square generates three variants. By choosing a reference state (e.g., the square state in the center of Fig. 1(a), or S1 in Fig. 1(b)), all the other vertices represent different structural states (or deformation states) with respect to the reference (Fig. 2(a)) and their connectivity can be determined through linear algebraic procedures [17], leading to the construction of a PTG (Fig. 2(b)). This PTG is infinite and interconnected, because the symmetry groups of the two phases (i.e., square and hexagonal) cannot be included in a finite common group [14]. Note that each structural state (corresponding to a vertex in the PTG) is uniquely determined associated with lattice correspondence, which could be in any orientation (parallel to the concept of objectivity or frame indifference in continuum mechanics) [22].

PTG is a theoretical framework to capture the connectivity of multiple structural states in different phases through transformation pathways, and all the accessible structural states during phase transformation cycles can be systematically determined. For example, starting from S1, HEX1 and HEX2 can be reached after a forward square to hexagonal transformation. During a backward transformation from hexagonal to square, HEX1 can transform to S1/S2/S3, while HEX2 can transform to S1/S4/S5. As a result, the structural states of S2-S5 could be reached after one transformation cycle, and more and more states can be reached after multiple transformation cycles [17]. All of the S2-S5 vertices are in the square lattice, but they are different structural states, which can be obtained by applying different lattice-invariant deformations on S1. Note that the description of transformation pathways in PTG is beyond the reach of Landau's phenomenological theory, in which a unique high-symmetry state that has all the symmetry elements of the low symmetry states is required. However, in the above 2D example of the transformation between square and hexagonal, a crystalline state having both four-fold and six-fold symmetry is theoretically impossible. The same is true for the FCC to BCC transformation through the Bain path, and the BCC to HCP transformation through the Burgers path [23, 24].

Grain boundary generation during the square to hexagonal transformation

Based on all the accessible structural states identified in the PTG, domain and defect structures generated during the square to hexagonal transformation can be systematically analyzed, with the incorporation of the geometric constraint (e.g., kinematic compatibility). For example, considering one transformation cycle (starting with S1) from square to hexagonal and back to square, the deformation gradient matrices for all the accessible states (S1-S5) can be determined, and the possible defect structures between the states of S1 and S2 can be predicted by solving kinematic compatibility condition [22, 25-28].

The deformation gradient matrices for structural states of S1, S2 and S5 are as follows [22, 27, 28]:

$$\mathbf{F}_{S1} = \begin{bmatrix} 1 & 0 \\ 0 & 1 \end{bmatrix}, \mathbf{F}_{S2} = \begin{bmatrix} 1 & 1 \\ 0 & 1 \end{bmatrix}, \mathbf{F}_{S5} = \begin{bmatrix} 1 & 0 \\ -1 & 1 \end{bmatrix} \tag{1}$$

Considering two neighboring grains (or domains) in different structural states (e.g., S1 and S2), we could expect a boundary between the two grains, and the type of the boundary as well as the misorientation between the two grains is dictated by the compatibility condition. For example, the defect structures between S1 and S2 are determined by [22, 25-28]:

$$\mathbf{Q}\mathbf{F}_{S2} - \mathbf{F}_{S1} = \mathbf{b} \otimes \mathbf{n} \tag{2}$$

where $\mathbf{Q}$ is a rigid-body rotation, $\otimes$ is the dyadic product. $\mathbf{b}$ and $\mathbf{n}$ are the shear vector and shear plane normal of a lattice invariant shear. The above equation is known as the Hadamard jump condition or invariant plane strain condition in continuum mechanics and phase transformation crystallography [22, 25-28]. $\mathbf{n}$ suggests the normal of a compatible grain boundary, while $\mathbf{Q}$ is the relative rotation between the two grains, which suggests the misorientation.

Two solutions of Eq. (2) can be obtained,

$$\begin{cases} \mathbf{b}_1 = \begin{bmatrix} 1 \\ 0 \end{bmatrix} \\ \mathbf{n}_1 = \begin{bmatrix} 0 \\ 1 \end{bmatrix} \end{cases}, \begin{cases} \mathbf{b}_2 = \frac{1}{5} \begin{bmatrix} -1 \\ 2 \end{bmatrix} \\ \mathbf{n}_2 = \begin{bmatrix} 2 \\ 1 \end{bmatrix} \end{cases} \tag{3}$$

which correspond to two different types of defect structures in the square lattice. The first solution suggests dislocations with Burgers vector of <10> on {01} plane. The second solution suggests a Σ5 GB on (21) plane with a misorientation of 53.13°. Note that the generation of coherent special GBs rather than general GBs could be expected because all the coherent special GBs are associated with certain symmetry operations in crystal lattice, which correspond to the broken symmetry during the phase transformation and transformation cycles.

With the knowledge of fundamental building blocks of structural states (e.g., S1-S5) determined by the PTG and the spatial relation among them (e.g., Σ5 boundary with 53.13° misorientation), self-organized multi-grain patterns can be constructed, which is parallel to the self-accommodation of martensite domain structures in shape memory alloys [22]. The formation of a possible self-accommodated multi-grain structure is shown in Fig. 2. In Fig. 2(a), it is a single crystal in S1 state before the transformation, and the regions indicated by different colors will go through different pathways during the transformation cycle. In Fig. 2(b), different grains shown by different colors are in different structural states or orientations. We should note the difference and connection between structural state and orientation. A grain in a given structural state could

be in any orientation (e.g., grains colored by light green and dark green are in S1 but different orientations), and two grains in different structural states could be in the same orientation (e.g., grains colored by orange and blue are in S2 and S5, respectively, but the same orientation). All the grains are in the square lattice in Fig. 2(b), so that all the boundaries are GBs. As shown in Fig. 2(b), there are three structural states (i.e., S1, S2 and S5) involved with only two different orientations. It is interesting to find that grains in S1 can exhibit both of the two orientations (the light green and dark green domains). The ones colored in light green are without rotation, while the ones colored in dark green are with 53.13° rotation. The grains in structural states of both S2 (orange) and S5 (blue) have the same orientation as that of the dark green grains, so that the boundaries among them (Σ1 GBs) cannot be distinguished in terms of lattice continuity (Fig. 2(b)). As a result, the whole multi-grain structure can be regarded as multiple isolated grains (light green) embedded in one large matrix grain (dark green, orange and blue). All the small isolated grains share the same misorientation of 53.13°, while all the GBs are Σ5 boundaries. Also note that such a multi-grain structure can periodically repeat to fill the whole space in 2D without any gap or overlap, which is critical for the formation of a compatible structure in macroscopic materials.

Note that this multi-grain structure produced through diffusionless phase transformation is unique in terms of geometry and topology. For conventional techniques in GB engineering, e.g., iterative cold working and annealing, it is difficult to precisely control the type of GBs, due to the high atomic mobility at annealing temperature. A large fraction of a specific type of GBs cannot be easily obtained unless there is an extremely strong GB energy anisotropy. In contrast, all the GBs produced through diffusionless phase transformation have to be coherent special GBs, the types of which are dictated by the broken symmetry during the phase transformation. In addition, such a unique topology, i.e., isolated small grains embedded in one matrix grain, is hard to obtain through annealing, because the GB energy will drive the shrinking of isolated small grains, when GB migration is allowed at elevated temperature. As the size of the isolated grain becomes smaller, the driving force (proportional to the GB curvature) becomes larger. As a result, it is difficult to stabilize nano-sized isolated grains at elevated temperature, even though they could lead to distinctive material properties (e.g., strength and ductility) [12]. However, as shown in Fig. 2(b), all the GBs are planar Σ5 boundaries, and the isolated grains can be stabilized due to very low mobility of special GBs at low temperature. In addition, because of the spatial correlation among the multi-grains (i.e., compatibility constraint), any diffusionless motion of the GBs will lead to the increase of either elastic energy (e.g., domain deformation) or grain boundary energy (e.g., coherent twins become incoherent). Given that Σ5 GBs are the special GBs with the lowest Σ value in square lattice (suggesting the maximal number of coincide lattice sites), the multi-grain structure shown in Fig. 2(b) is stable at low temperature (diffusional GB migration is not allowed). Note that such a mechanism suggests a new way to produce stabilized nano-grain structure, and the size of the isolated grains is determined by the interplay of GB energy and elastic interaction energy (if the GB energy is larger, the grain size becomes larger),

which is parallel to the formation of modulated nano-domain structures during structural phase transformations [22, 28].

The above example in 2D is informative to illustrate the crystallographic origin of multi-grain structures (with coherent special GBs) generated by phase transformation cycling. It also establishes the theoretical foundation to describe this phenomenon. From a mathematical point of view, Fig. 2 provides a way to fill a space completely with several specific types of building blocks without any gap or overlap. The building blocks are associated with the nature of the phase transformation, i.e., symmetry breaking. The way the building blocks arrange themselves is constrained by the compatibility among different domains, e.g., Eqn. (1)-(3), which can be easily understood through Fig. 2.

Design of self-organized multi-grain structures in BCC crystal

As shown in the above 2D example of the square to hexagonal transformation, a unique isolated grain structure can be constructed by an appropriate choice of structural states (i.e., S1, S2 and S5). Those structural states could be self-organized due to compatibility (or elastic interaction), which suggests a thermodynamic feasibility of the formation of such a multi-grain structure. However, we can also expect kinetic difficulties in this process. During the transformation from square to hexagonal, structural states of HEX1 and HEX2 are crystallographically and energetically equivalent (Fig. 1). So, we expect an equal probability of the formation of domains in HEX1 and HEX2 states. During the backward transformation from hexagonal to square, for the domains starting with HEX1, there is an equal probability to reach S1, S2 and S3. Similarly, the domains starting with HEX2 have an equal probability to reach S1, S4 and S5. As a result, after a whole transformation cycle, the final probabilities that a grain is in the structural state of S1, S2, S3, S4, S5 could be simply estimated as 1/3, 1/6, 1/6, 1/6, 1/6, respectively (by ideal random selection without considering the spatial correlation among multiple domains). Considering the grain structure formed in Fig. 2, we only need S1, S2 and S5 in particular, which could be difficult to be achieved in such a "random walk" process (random walk of structural state in PTG). In other words, in order to obtain the unique grain structure shown in Fig. 2, a strong bias preferring S2 and S5 (over S3 and S4) should be applied. The bias could be some kind of external field. For a general design strategy of the bias, we will take a real material system, where the physical nature of the phase transformation determines the type of the bias.

Real material systems in 3-dimensional (3D) space are rather complex. Five degrees of freedom of GBs in 3D space provides more choices of special GBs during phase transformation cycling. Here we consider a transformation cycle between BCC and HCP through the Burgers path, which is typically found in Ti and Zr alloy systems. Note that the symmetry groups of BCC and HCP cannot be included in a common finite group, because a crystalline state with both four-fold and six-fold rotational symmetry is theoretically impossible. As reported in the literature [21],

starting from one BCC state, twelve crystallographically equivalent HCP states can be generated through the Burgers path, which can be divided into six shear modes. The two HCP states within the same shear mode have opposite internal shuffles, which lead to different stacking sequence along [0001] direction (i.e., one HCP has ABAB… stacking sequence while the other has ACAC… stacking sequences). In our following analysis, these two HCP states within the same shear mode will not be distinguished (described by one vertex in PTG), since they are exactly the same in terms of both crystal orientation and shear mode. During the reverse transformation from HCP to BCC, three crystallographically equivalent BCC states are generated due the loss of the three-fold rotational symmetry in HCP.

The PTG for the BCC to HCP transformation is shown in Fig. 3. Each BCC state is neighbored with six HCP states (6 shear modes), while each HCP state is neighbored with three BCC states. Starting from B1, we can get another twelve BCC states, i.e., B2-B13, after a transformation cycle. All of the BCC states can be taken as building blocks to construct a self-accommodated multi-grain structure. Here we choose four BCC states, i.e., B2-B5, and the deformation gradient matrices for those states are as follows (B1 is chosen as the reference state, i.e., the identity deformation gradient matrix),

$$\mathbf{F}_2 = \begin{bmatrix} 0.75 & -0.25 & -0.5 \\ -0.25 & 0.75 & -0.5 \\ 0.75 & 0.75 & -0.5 \end{bmatrix}, \mathbf{F}_3 = \begin{bmatrix} 0.75 & -0.25 & 0.5 \\ -0.25 & 0.75 & 0.5 \\ -0.75 & -0.75 & -0.5 \end{bmatrix},$$
$$\mathbf{F}_4 = \begin{bmatrix} 0.75 & 0.25 & 0.5 \\ 0.25 & 0.75 & -0.5 \\ -0.75 & 0.75 & 0.5 \end{bmatrix}, \mathbf{F}_5 = \begin{bmatrix} 0.75 & 0.25 & -0.5 \\ 0.25 & 0.75 & 0.5 \\ 0.75 & -0.75 & 0.5 \end{bmatrix} \quad (4)$$

Both the crystallographic analysis and the phase field simulations suggest that grains in B2-B5 states can form a self-accommodated cross-twin structure as shown in Fig. 4 [29]. The atomic structure is visualized using the Ovito software [30]. Grains in different structural states are plotted in different colors (blue: B2; green: B3; yellow: B4; red: B5). For this structure, it can be found that all the GBs between different grains are coherent special GBs. The cross-twin structure can also be regarded as "twins within twins". As shown in Fig. 4, blue and green grains with Σ3 boundaries (also yellow and red grains) form 1st-level twins, while (blue/green) and (yellow/red) grains with Σ7 boundaries form 2nd-level twins.

Even though both the crystallographic analysis and the phase field simulation suggest the stability of such a cross-twin structure, an engineering design to precisely select the four domain states (i.e.,g B2-B5) is still required. Since the BCC to HCP transformation is a typical phase transformation in response to a stress field, we expect that a biased stress could serve the purpose. The transformation strains for the structural states of B2-B5 can be determined through Lagrangian finite strain formula,

$$\mathbf{E}_i = \frac{\mathbf{F}_i^T \mathbf{F}_i - I}{2}, i = 2 \sim 5 \quad (5)$$

$$\mathbf{E}_2 = \begin{bmatrix} 0.09375 & 0.09375 & 0.0625 \\ 0.09375 & 0.09375 & 0.0625 \\ 0.0625 & 0.0625 & -0.125 \end{bmatrix}, \mathbf{E}_3 = \begin{bmatrix} 0.09375 & 0.09375 & -0.0625 \\ 0.09375 & 0.09375 & -0.0625 \\ -0.0625 & -0.0625 & -0.125 \end{bmatrix},$$

$$\mathbf{E}_4 = \begin{bmatrix} 0.09375 & -0.09375 & -0.0625 \\ -0.09375 & 0.09375 & 0.0625 \\ -0.0625 & 0.0625 & -0.125 \end{bmatrix}, \mathbf{E}_5 = \begin{bmatrix} 0.09375 & -0.09375 & 0.0625 \\ -0.09375 & 0.09375 & -0.0625 \\ 0.0625 & -0.0625 & -0.125 \end{bmatrix},$$

(6)

From the above transformation strains, it is clear that a uniaxial compressive stress along the [001] direction is the most convenient biased-load condition to make exactly the desired four BCC states (i.e., B2-B5) energetically favorable. And it can be easily shown that such a uniaxial stress will not favor B6-B13.

As reported in the literature, cross-twin structures are commonly observed in low-symmetry phases (e.g., orthorhombic and monoclinic) during diffusionless phase transformations, as a result of autocatalytic nucleation and self-accommodation [19, 22, 28, 31]. In such cases, the structural states in low-symmetry phases are within a single EPN. By designing a cross-twin in a high-symmetry (i.e., BCC) phase with the structural states in multiple EPNs involved, we also suggest a thermo-mechanical process to generate the multi-grain structure in Fig. 4, i.e., a thermal transformation cycling with a uniaxial compressive biased-load. The microstructure evolution during the transformation cycling is illustrated schematically in Fig. 5 and the atomic structure are shown in Fig. 6. Starting from a single crystal in B1 state at high temperature, a uniaxial compressive biased-load is applied and maintained during the whole thermal cycling process. When the system is quenched to low temperature, HCP becomes the stable phase. Two HCP variants, in H1 and H2 states, are energetically favored (over H3-H6) by the biased-load, leading to a $\{10\bar{1}2\}$ type of twin in HCP. Thereafter, the system is heated to high temperature, and BCC becomes the stable phase again. During the heating, each HCP domain has three choices. It can either go back to the initial BCC state or transform to new BCC states, e.g., the domain in H1 state can transform to B1, B2 or B3 state. Since the biased-load makes all the four new BCC states (i.e., B2-B5) energetically favorable, the HCP domains would prefer to transform to the new BCC states. As a consequence, the $\{10\bar{1}2\}$ type of twin boundaries in HCP becomes a special type of GBs (Σ7 boundaries) in BCC, and a new type of grain boundaries (Σ3 boundaries) can be generated, since the biased-load equally favors the four structural states of B2-B5. In ideal case, the whole process does not produce internal stress when the designed microstructure forms (i.e., microstructures in Fig. 5), as proven by our crystallographic analysis. During the whole transformation cycle, the macroscopic shape of the system changes, i.e., it elongates along [100], [010] directions and contracts along [001] (due to the biased-load), generating the following averaged strain (if the volume fractions of all the four kinds of domains are 25% [29]),

9

$$\mathbf{E}_{ave} = \frac{\mathbf{F}_{ave}^T \mathbf{F}_{ave} - \mathbf{I}}{2} = \begin{bmatrix} 0.08333 & 0 & 0 \\ 0 & 0.07143 & 0 \\ 0 & 0 & -0.125 \end{bmatrix} \tag{7}$$

Theoretically, the volume fractions of the four kinds of domains are adjustable with the constraint: $f_{B2} : f_{B3} = f_{B5} : f_{B4}$, which could change the averaged strain as well.

With the deformation gradient matrix for each domain calculated, the atomic structure during lattice distortion can be generated using Ovito [30]. The formation mechanism of special GBs generated by transformation cycling is shown in Fig. 6. All the domain states are referred to the structural state in Fig. 3. Starting from a single crystal in B1 state, a $\{10\bar{1}2\}$ twin forms during the BCC to HCP transformation. To satisfy the compatibility condition, there is a rotation of 3.37° between H1 and H2 domains, so that the twin boundary (dashed line) is not horizontal in Fig. 6. In addition, the relaxation of a number of atoms near the twin boundary (the green atoms near the dashed line) will be expected, which is parallel to the local relaxation during the formation of $\{10\bar{1}2\}$ deformation twin in HCP structures. A subsequent transformation from HCP to BCC produces the cross-twin structure with Σ3 and Σ7 GBs. We also choose another convenient viewing direction (a common <111> for B2-B5 domains), shown in the second row of Fig. 6. Considering the difference between the initial and final structures, the initial one is a single crystal while the final one is a multi-grain structure with a macroscopic shape change (Eqn. (7)). Note that both the initial and the final structure can periodically repeat to fill the whole space in 3D, without any gap or overlap.

The change of atomic structure in a single domain is shown in Fig. 7 to further illustrate the mechanism clearly. The domain undergoes a B1 to H1 to B2 transformation cycle (referred to the structural state in Fig. 3). The viewing directions for the upper and lower rows are $[00\bar{1}]$ and $[\bar{1}10]$, respectively, in B1 index. In H1 state (second column), there is a six-fold rotational symmetry with a rotation axis of $[0001]_{H1}/[\bar{1}10]_{B1}$. B1 and B2 are two crystallographically equivalent structural states with respect to H1, and they can be connected by a lattice-invariant deformation. As a result, the macroscopic shape of this domain changes during the transformation cycle. In general, all the domains should have cooperative shape changes (or self-accommodation) to avoid internal stress and the generation of dislocations.

The $\{10\bar{1}2\}$ type of twin structures formed during the BCC to HCP transformation have been widely observed in experiments, with a typical domain size of hundreds of nanometers [32]. In addition, coherent special GBs, e.g., Σ3 and Σ11 (characteristic GBs between domain states of B1 and B2), are also observed during the BCC to HCP transformation cycling in Ti-alloys and the α to ε transformation in Fe-alloys induced by either temperature or stress [33-37]. With the above necessary pieces, the formation of cross-twin structures should also be expected with an

elaborated processing design. Up to now, there is no direct experiment with the thermo-mechanical processing as we suggest, so the cross-twin structure in BCC has not been observed yet. Since the mechanism we propose requires an interdisciplinary knowledge of crystallography and phase transformation within a new mathematical framework (beyond the reach of Landau's theory), PTG, it is rather difficult to elucidate without a theoretical guideline. Also note that the energetic competition between GBs and dislocations are not considered in the above, which is beyond the scope of crystallography analysis. As observed in experiments, both dislocations and GBs can be generated by transformation cycling [18, 20, 33]. We have a few suggestions regarding this competition from a crystallographic point of view. Firstly, when the symmetry of the product phase is reduced, e.g., HCP is reduced to orthorhombic (orthorhombic is a subgroup of BCC), twin could become dominant over dislocations. In experiments, the HCP phase in Ti can change to α'' (orthorhombic) by introducing alloy additions (e.g., Mo, Nb, etc.), which leads to twin-dominant microstructures during the transformation [32]. A similar phenomenon of twin/dislocation competition is also reported in Fe alloys with carbon addition (i.e., steels). A relatively low temperature is preferred, which kinetically favors twinning over dislocation. Secondly, the geometric features of the cross-twin structure (e.g., all compatible boundaries and spatial periodicity) are critical for the nucleation, growth and the self-organization of multiple domains [29], because of the macroscopic shape change. As reported in the literature, the cross-twin domain structures are widely observed in experiments as a self-accommodated microstructure [19, 22, 28, 31], which strongly suggests the feasibility of such a self-organization process. In addition, a volume change as small as possible (e.g., <1%) during the transformation is also required. Otherwise, dislocations will be induced inevitably during the transformation. Thirdly, a low level of biased-load during the forward transformation is preferred, which assists the pathway selection but does not activate the possible symmetry-dictated non-phase transformation pathway [17, 18]. In contrast, a relatively high level of biased-load is required during the backward transformation to drive the domains to new structural states rather than the original. However, the biased-load stress should be always lower than the yield strength of either the parent or the product phase. Fourthly, the same mechanism shown in Fig. 5 will not be limited within BCC/HCP transformation. For example, the transformation between γ (BCC) and α (face-centered orthorhombic) in uranium-alloys shares similar broken symmetry. As a result, the cross-twin structure with $\Sigma3$ and $\Sigma7$ (Fig. 4) can also be expected during the transformation cycling in uranium alloys. Theoretically, $\{10\bar{1}2\}$ type deformation twins in HCP (similar to the structure in the middle of Fig. 5) could also produce the cross-twin structure after a transformation to BCC (with appropriate biased-load), which is a one-way transformation rather than cycling.

Besides the system of the BCC to HCP transformation presented above, a few general strategies to select other material systems to produce special GBs can also be suggested. A reconstructive phase transformation (the symmetry groups of the parent and product phases cannot be included in a common finite group) is required to generate multiple structural states, which are the

11

necessary building blocks to generate multiple grains as well as GBs among them. A self-accommodated multi-grain structure is also required for vanishing elastic strain and internal stress, which is critical to prevent plastic yielding and dislocation generation. A self-accommodated structure is related to the symmetry change, while a volume change as small as possible during the phase transformation is another critical factor to reduce internal stress and prevent dislocation plasticity. An energy-based model should be required to quantify the competition between GBs and dislocations. However, it is beyond the scope of our current crystallographic analysis. Theoretically, the conventional Landau phase transition theory cannot capture the nature of the mechanism we propose. Instead, order parameters associated with translational symmetry [38, 39] should be employed to describe the cycling process of reconstructive phase transformations.

Here we summarize the major procedures in designing and synthesizing unique multi-grain structures and special GBs through diffusionless phase transformation cycling:

(1) Select a material system with a structural phase transformation, in which the symmetry groups of the parent and product phases cannot be included in a common finite group;
(2) Construct the PTG and identify possible structural states during transformation and transformation cycles (similar to Fig. 3);
(3) By utilizing the structural states in the PTG as building blocks, construct a self-accommodated multi-grain (i.e., polycrystalline) structure with coherent special GBs (similar to Fig. 4);
(4) Select an appropriate external field to make the necessary structural states (or building blocks) energetically favorable;
(5) Suggest a formation process of the multi-grain structure according to the transformation pathways in the PTG (similar to Fig. 5).

Conclusion

We propose a new mechanism to produce special grain boundaries through diffusionless phase transformation cycling. Both the geometric character of grain boundaries and the topology of grain boundary network produced in this way are unique, which could lead to favorable material properties. Comparing with conventional methods in grain boundary engineering, the following distinctions of the method presented in this work should be noted:

(1) All the grain boundaries are coherent special grain boundaries, the types of which are dictated by the broken symmetry during the phase transformations;

(2) The topology of the grain boundary network is determined by the spatial correlation of the multi-grain structure, which can be precisely designed and controlled by applying external fields during the phase transformations;

(3) The multi-grain structures are free of internal stress (in ideal case);

(4) A new theoretical framework, phase transition graph, is employed to investigate the generation of grain boundaries during phase transformations, which is beyond the reach of Landau's phase transition theory;

(5) The work suggests a new methodology for a precise design and synthesis of coherent special grain boundaries, with a grain size at the nano/submicro-scale.

Reference:

[1] G. Palumbo, E.M. Lehockey, P. Lin. J Min. Met. Mat. S. **50**, 40 (1998).

[2] V. Randle. Mater. Sci. Technol. **26**, 253(2010).

[3] D.G. Brandon. Acta Metall. **14**, 1479 (1966).

[4] C.A. Schuh, M. Kumar, W.E. King. Acta Mater. **51**, 687 (2003).

[5] R. Raj, M.F. Ashby. Metall. Trans. **2**, 1113 (1971).

[6] J. W. Cahn, J. E. Taylor. Acta Mater. **52**, 4887-4898 (2004).

[7] E. O. Hall. Proc. Phys. Soc. London **64**, 747 (1951).

[8] N. J. Petch, N.J. J. Iron Steel Inst. London **173**, 25 (1953).

[9] N. Ma, S. A. Dregia, Y. Wang. Acta Mater. **51**, 3687 (2003).

[10] M. Tang, B. W. Reed, M. Kumar. J. Appl. Phys. **112**, 043505 (2012).

[11] V. Randle. Acta Mater. **52**, 4067 (2004).

[12] X. Wu, F. Yuan, M. Yang, P. Jiang, C. Zhang, L. Chen, Y. Wei, E. Ma. Sci Rep. **5**, 11728 (2015).

[13] L. Lu, Y. Shen, X. Chen, L. Qian, K. Lu. Science **304**, 422 (2004).

[14] K. Bhattacharya, S. Conti, G. Zanzotto, J. Zimmer. Nature **428**, 55 (2004).

[15] L.D. Landau, Phys. Z. Sowjetunion **11**, 545 (1937).

[16] J.L. Ericksen. Arch. Ration. Mech. Anal. **73**, 99 (1980).

[17] Y. Gao, S. A. Dregia, Y. Wang. Acta Mater. **127**, 438 (2017).

[18] M. L. Bowers, Y. Gao, L. Yang, D.J. Gaydosh, M. De Graef, R.D. Noebe, Y. Wang, M.J. Mills. Acta Mater. **91**, 318 (2015).

[19] M. Nishida, H. Ohgi, I. Itai, A. Chiba, K. Yamauchi. Acta Metall. **43**, 1219 (1995).

[20] Y. Gao, L. Casalena, M. L. Bowers, R. D. Noebe, M. J. Mills, Y. Wang. Acta Mater. **126**, 389 (2017).

[21] Y. Gao, R. Shi, J.-F. Nie, S. A. Dregia, Y. Wang. Acta Mater. **109**, 353 (2016).

[22] K. Bhattacharya, *Microstructure of Martensite: Why it Forms and How it Gives Rise to the Shape Memory Effect* (Oxford Univ. Press, Oxford, UK, 2003).

[23] E. C. Bain. Trans. AIME, **70**, 25 (1924).

[24] W. G. Burgers, Physica **1**, 561 (1934).

[25] B. M. Wechsler, D. S. Lieberman, T. A. Read, Trans. AIME **197**, 1503 (1953).

[26] J. K. Mackenzie, J. S. Bowles, Acta Metall. **2**, 138 (1954).

[27] C. M. Wayman, *Introduction to the crystallography of martensitic transition* (Collier-Macmillan, New York, USA, 1964).

[28] A. G. Khachaturyan, *Theory of Structural Transformations in Solids* (Wiley, New York, USA, 1983).

[29] See Supplemental Material at [URL will be inserted by publisher] for crystallographic calculations and phase field modeling.

[30] A. Stukowski. Modelling Simul. Mater. Sci. Eng. **18**, 015012 (2010).

[31] M. Nishida, K. Yamauchi, I. Itai, H. Ohgi, A. Chiba. Acta Metall. **43**, 1229 (1995).

[32] Z. Nishiyama, *Martensitic Transformation*, Academic Press, London, 1978.

[33] M. J. Lai, C. C. Tasan, D. Raabe. Acta Mater. **111**, 173 (2016).

[34] P. Castany, Y. Yang, E. Bertrand, T. Gloriant. Phys. Rev. Lett. **117**, 245501 (2016).

[35] L. M. Dougherty, G. T. Gray III, E. K. Cerreta, R. J. McCabe, R. D. Field, J. F. Bingert. Scr. Mater. **60**, 772 (2009).

[36] S. J. Wang, M. L. Sui, Y. T. Chen, Q. H. Lu, E. Ma, X. Y. Pei, Q. Z. Li, H. B. Hu. Sci. Rep. **3**, 1086 (2012).

[37] J. W. Christian, S. Mahajan. Deformation twinning. Prog. Mater. Sci. **39**, 1 (1995).

[38] P. Toledano, V. Dmitriev. *Reconstructive phase transitions in crystals and quasicrystals* (World scientific publishing Co. Pte. Ltd., Singapore, 1996).

[39] V. P. Dmitriev, S. B. Rochal, Y. M. Gufan, P. Toledano. Phys. Rev. Lett. 60, 1958 (1988).

[40] Y. Wang, A. G. Khachaturyan. Acta Mater. **45**, 759 (1997).

[41] Y. Gao, N. Zhou, D. Wang, Y. Wang. Acta Mater. **68**, 93 (2014).
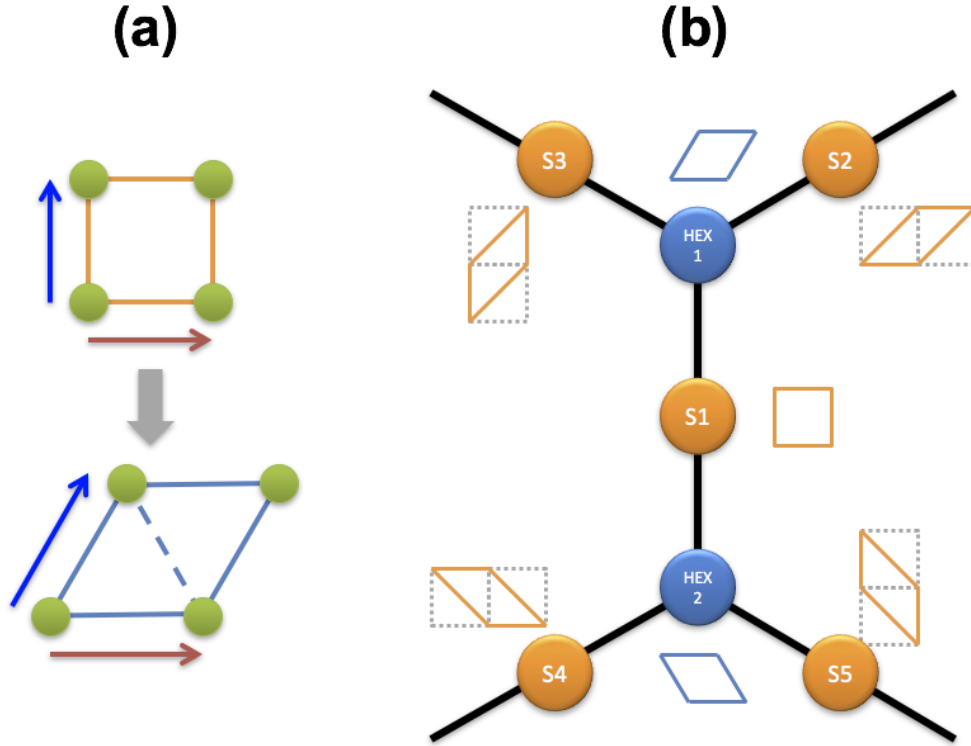
Fig. 1. Construction of the phase transition graph for a square to hexagonal transformation: (a) change of crystal structure; (b) vertices and edges in PTG. (Blue and dark red lines in (a) represent two independent vectors in the 2D lattices and they also indicate the lattice correspondence among all the structural states in (b)). The orange shapes in (b) indicate lattice-invariant deformations of original square lattice S1 and the corresponding new square lattices are represented by dotted lines.
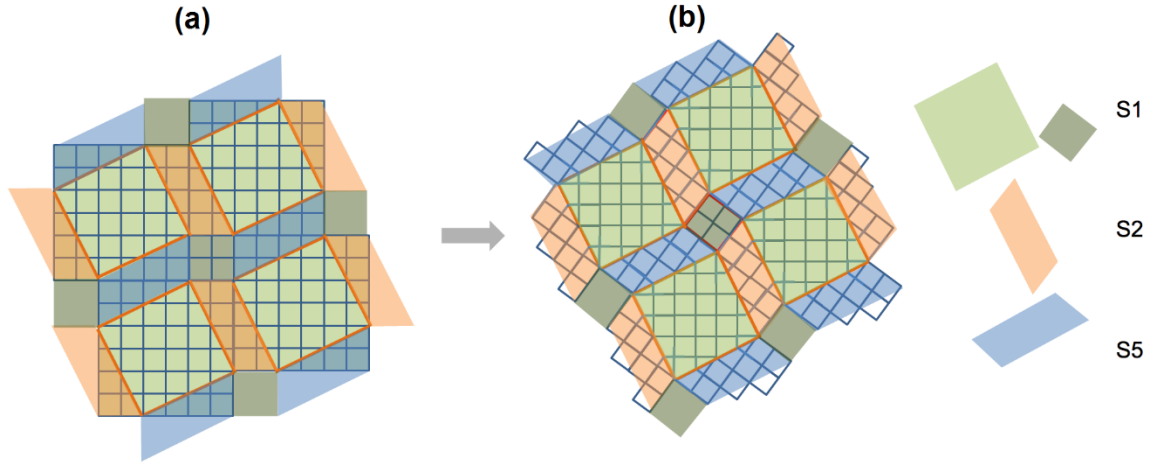
Fig. 2. Multi-grain structure produced through a square to hexagonal transformation: (a) single grain in S1 state before phase transformation; (2) a multi-grain structure with S1, S2 and S5 domain states after one forward-backward transformation cycle. See Fig. 1 for S1, S2 and S5 structural states of the square phase.
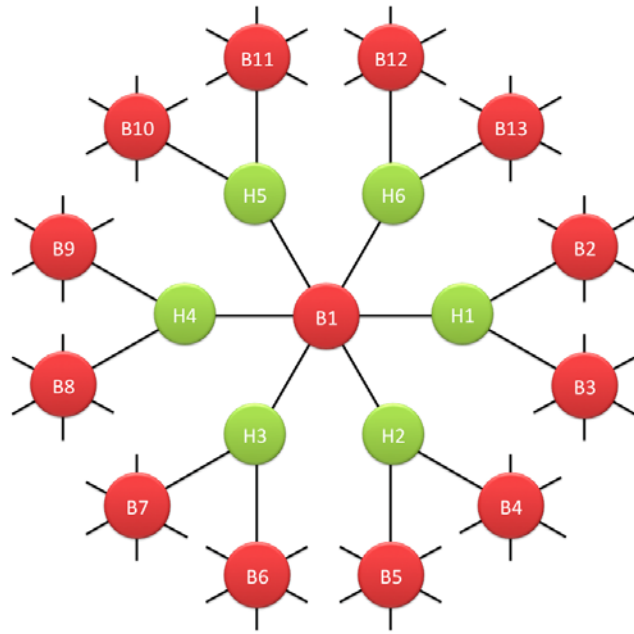
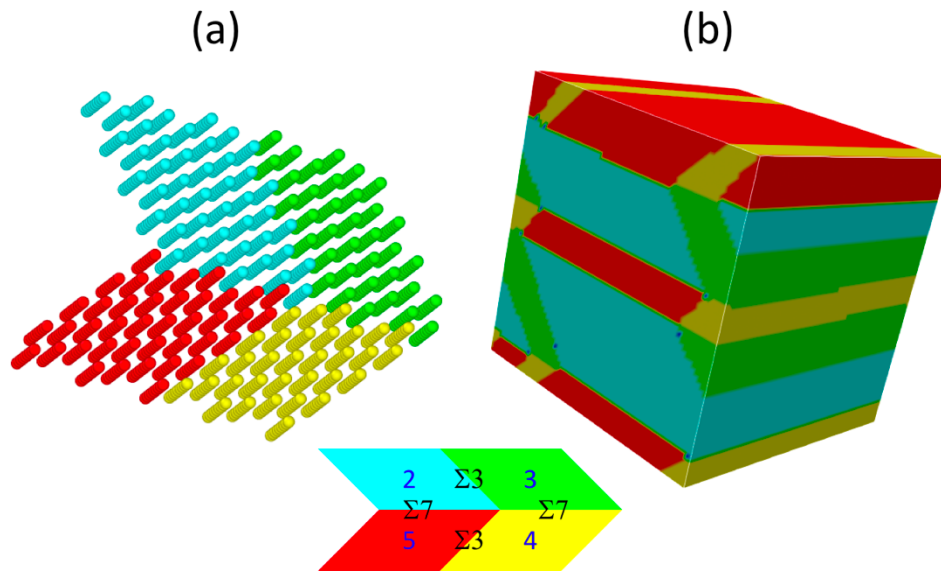Fig. 3. PTG for the BCC to HCP transformation.

Fig. 4. A cross-twin multi-grain structure formed in BCC: (a) atomic structures; (b) phase field simulation result.
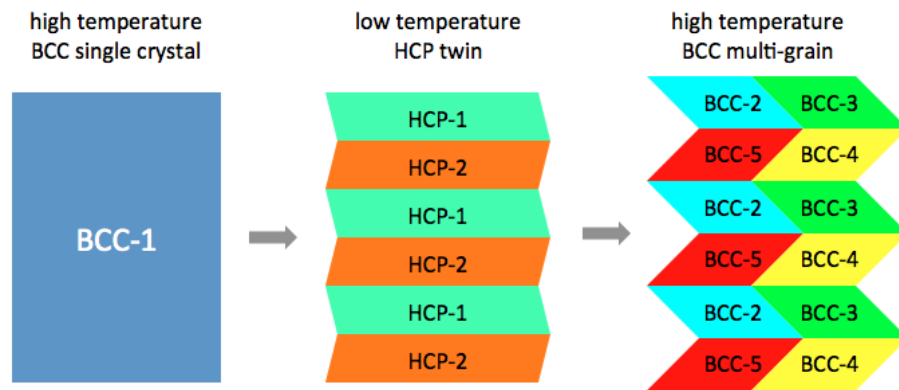
Fig. 5. Schematic drawing of the formation process of multi-grain pattern in BCC through biased-load thermal cycling.
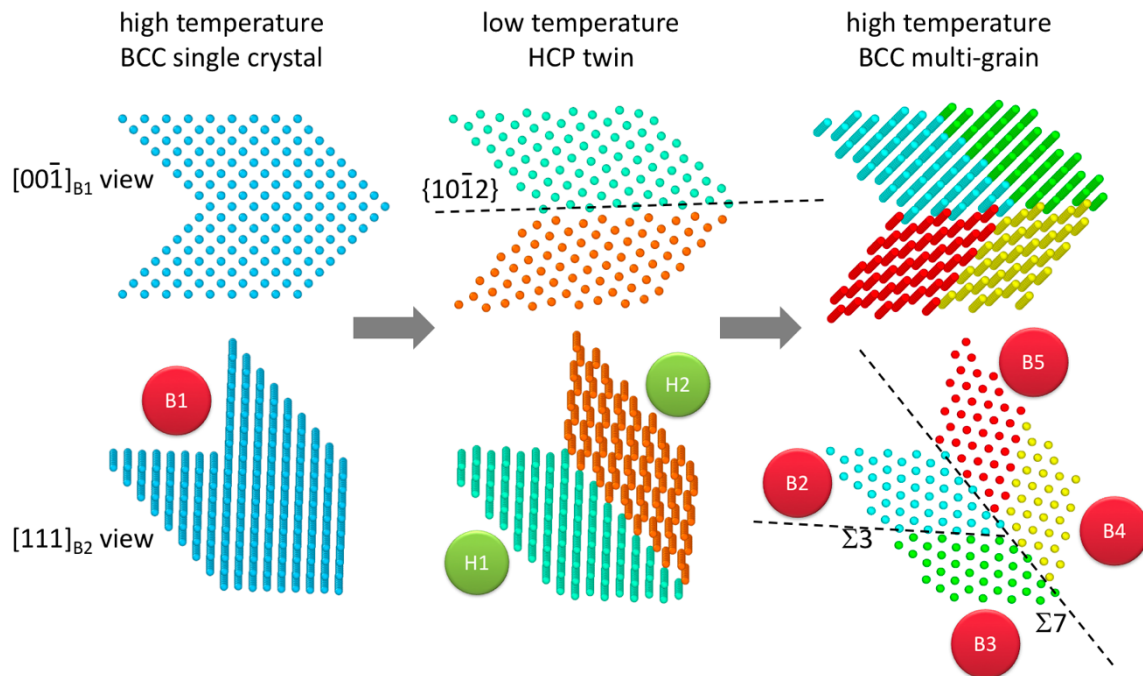
Fig. 6. Atomic structure for the formation of multi-grain pattern in BCC during transformaiton cycling.
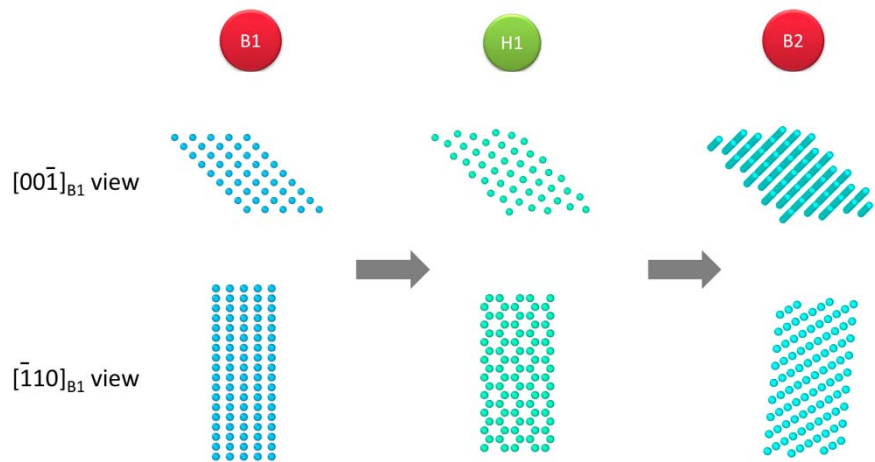
Fig. 7. Lattice distortions in B2 domains during transformation cycling.